Evaluation of Spherical Particle Sizes With an Asymmetric Illumination Microscope

Jessica C. Ramella-Roman, Paulo R. Bargo, Scott A. Prahl, and Steven L. Jacques

***Abstract*—A polarized microscope system is used to perform goniometric measurements of light scattered by small particles. The light incident angle on a sample of monodispersed latex microspheres is increased sequentially and a microscope objective lens collects scattered light from the samples. Light is only collected at angles greater than the objective lens numerical aperture (NA) so that only light scattered by the spheres is collected. The experimental results were modeled with a Mie theory-based algorithm. Experiments conducted with microspheres of diameter 1.03, 2.03, and 6.4 μm show that, by decreasing the objective lens NA from NA $= 0.55$ to NA $= 0.0548$, a more distinguishable scattering pattern is detectable. From these highly shaped curves, we found that the size of a sphere of nominal diameter 2.03 μm was 2.11 $\pm$0.06 μm and a 6.4 μm sphere was 6.34 $\pm$0.07 μm.**

***Index Terms*—Asymmetric illumination, goniometry, Mie theory, oblique microscopy, polarized light microscopy.**

I. Introduction

MORPHOLOGICAL changes in cell nuclei can indicate a precancerous state, and for this reason many studies have tried to characterize cell nuclei as means of early cancer diagnosis [1]–[6]. Backmann and Perelman [1], [2] developed a polarized light spectroscopic method to quantitatively measure epithelial cell structure *in situ*, and in particular the nuclear size and relative refractive index. They distinguished healthy from cancerous mucosal tissue by determining the size distribution of epithelial cell nuclei: cancerous epithelial nuclei are dysplastic and larger than normal nuclei.

Richards-Kortum *et al.* [3] used similar techniques to measure cell nuclei sizes and indices of refraction. These spectroscopic techniques could lead to noninvasive early detection of epithelial cancer, which constitutes 90% of all cancers.

Canpolat and Mourant [4] developed a fiber optic probe for particle size analysis in turbid media. They used a single fiber for delivery and collection and matched their results to Mie theory and Monte Carlo models.

In microscopy, Ovryn and Khaydarov [5], [6] developed a method to assess the location of the scattering spheres in three-dimensional flows. They spatially resolved the detailed structure of the scattered light from spherical particles in tenuous media, using a high numerical aperture (NA) microscope and a single wavelength. They were able to apply their model to the measurement of cell nuclei size using a reference library of scattering patterns from known particles, matching the theoretical patterns to experimental ones with a neural network.

Our experiment focused on the first important issue to solve when determining particle size: the determination of a particle size in a monodisperse solution. We used an inverted microscope and a goniometric assembly that directed monochromatic light onto the scattering particle at different angles. We used a cooled charge-coupled device (CCD) camera to capture images of scattering patterns from a single latex micro sphere. Microspheres of different sizes were measured.

The goal of this technique is to enrich an image of small particles obtained with a high magnification microscope by adding specific information on particle size which are not easily obtainable with a microscope alone. This would be particularly helpful in sizing subcellular structures and in detecting changes in cell morphology *in vivo*.

We developed a model to determine the particle size when the relative index of refraction is known.

Asymmetric illumination contrast (AIC) has been used in microscopy [7], [8] in the past to enhance image contrast, but was largely abandoned after the invention of phase contrast microscopy. More recently, AIC has been used for three-dimensional imaging of cellular structures [9]. Our method differs from AIC by the use of only angles of incidence above the objective lens NA, so that unscattered light is not collected, and only light scattered by the particle is collected. Unlike AIC, our goal was not to enhance contrast, but to use the angular information to build a particle phase function. We used this method to measure the size of latex microspheres ranging from 1.03 to 6.4 μm.

II. Materials and Methods

An inverted microscope (Eclipse TS100, Nikon, Mellville, NY) was modified by replacing the original light source with a goniometric assembly to allow illumination at arbitrary angles. A 16-bit CCD camera (Princeton Scientific, Trenton, NJ) was mounted on the microscope to collect high-resolution images.

The goniometric light source assembly is shown in Figs. 1 and 2. Light was delivered from a 630-nm dye laser and pumped to the microscope by a frequency-doubled Nd–YAG laser (Laserscope, San Jose, CA) through an optical fiber with a core diameter of 0.6 mm. To remove speckle and improve image quality, the optical fiber was shaken with an aquarium pump. The incident angle of the beam was adjusted by positioning the fiber at different angles. We considered the range of angles from θ_c ($\sin^{-1}$ NA $= 33.7°$) to 80°. To center the beam in the sample plane for every incident angle, the optical fiber was mounted

Manuscript received November 18, 2002; revised February 3, 2003. This work was sponsored by the National Institute of Health under Grant RO1-CA80985 and Grant R24-CA84587.

The authors are with the Oregon Health and Sciences University, Portland, OR 97225 USA (e-mail: sjacques@ece.ogi.edu).

Digital Object Identifier 10.1109/JSTQE.2003.811289

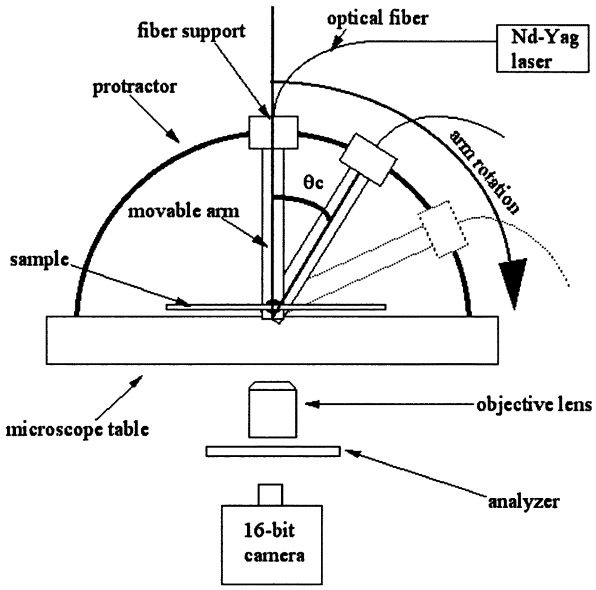

Fig. 1. Front view of the goniometric assembly. The optical fiber rotates around a pivotal point; the fiber is mounted on a Delrin arm. The exact angular position of the incident beam is measured with a protractor.

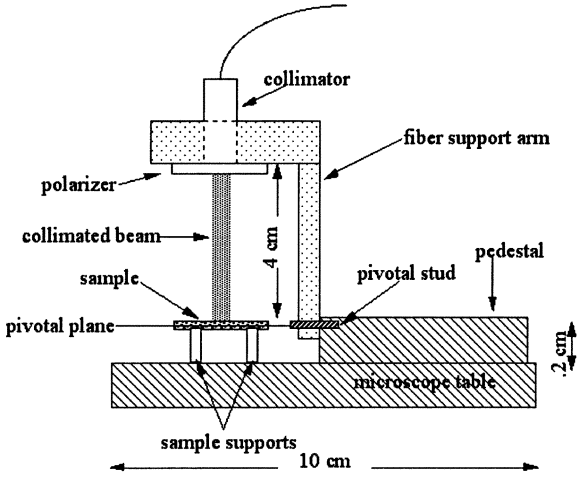

Fig. 2. Detail of the fiber support arm. The laser spot is centered on the pivotal plane for every θ angle of the support arm. The sample is maintained at the center of the pivotal plane with glass supports. A pedestal connected to the microscope table with double-sided tape assures the rigidity of the system.

on an arm connected at its pivotal point to a pedestal. A microlens assembly collimated the light beam; spot size was approximately 4 mm in diameter. The sample was composed of latex microspheres (Ted Pella, Redding, CA; Duke Scientific, Palo Alto, CA; Bangs Laboratories, Fishers, IN) in a diluted aqueous solution, sandwiched between glass slides and positioned, with glass supports, in the center of the pivotal plane. The index of refraction of the micro sphere was 1.59 and the index of refraction of the aqueous solution was 1.33. Angles were measured with a protractor.

The incident light was linearly polarized with a polarizer (Hinds, Portland, OR). An analyzer, positioned behind the microscope objective lens, selected only one polarization state. The extinction ratio of the polarizer analyzer pair was 1:10 000. During experiments the polarizer and analyzer were either both parallel or both perpendicular to the plane of incidence. For

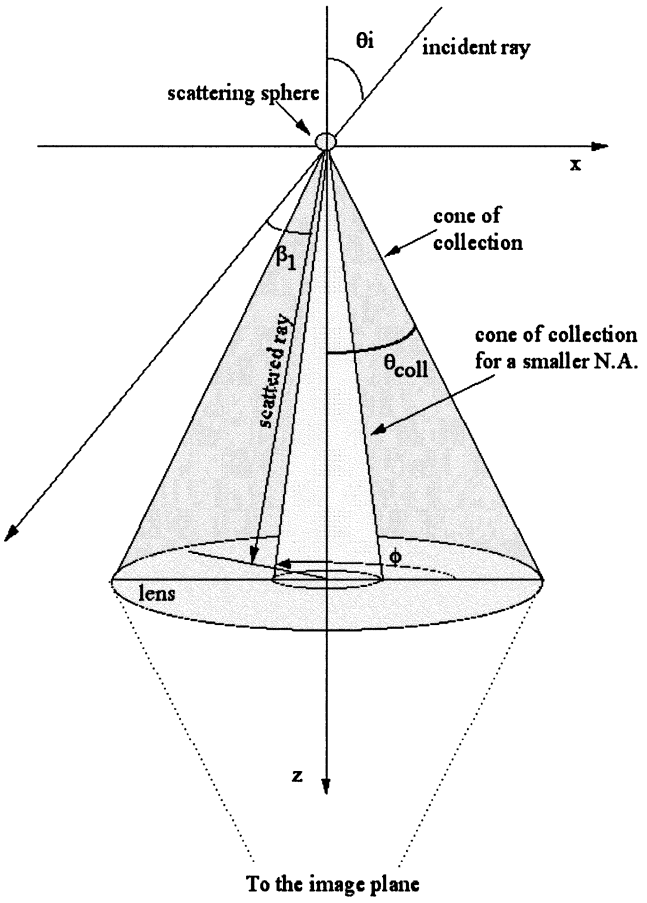

Fig. 3. Collection model. The NA of the objective lens is defined as NA $= n\sin(\theta)$. The direction of propagation is z.

every arm position, IPlab software captured an image of the sample. Acquisition time was one second. The objective lens used for all the experiments was a 40× magnification objective with 0.55 NA; the working distance of the objective lens was 2.1 mm.

A. Image Evaluation

For each particle size, we captured a minimum of one image for every 5° of illumination angles. All images were analyzed with Matlab software. To account for the camera's intrinsic dark noise, a dark noise value of $\sim$ 460 counts was subtracted from every image. The individual microspheres stood out in the captured images as bright round circles. For nonperpendicular illumination, the microspheres exhibited this circular shape, but with a bright tail; this tail was not considered during the analysis. To analyze the images, we sampled a region of interest (ROI) of ± 4 pixels around the center (X_o, Y_o) of the sphere circular image. The mean of the ROI was calculated and plotted versus the incident angle θ. This process was repeated for three spheres on the same image.

B. Collection Model

We implemented a simple model based on Mie scattering. The model incorporated the NA of the objective lens so its ability to collect light-rays scattered by the micro sphere was accurately simulated. Fig. 3 shows the geometry of the

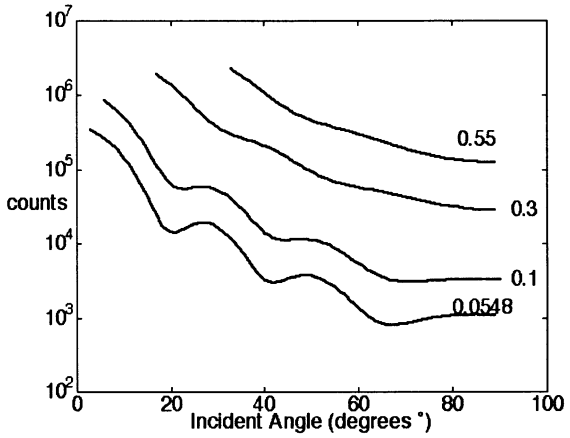

Fig. 4. Modeled behavior of perpendicular polarized incident light and perpendicular collection by a microscope objective lens of increasing NA for spheres of diameter $= 2.03$ μm. The plotted NAs are 0.0548, 0.1,0.3, and 0.55.

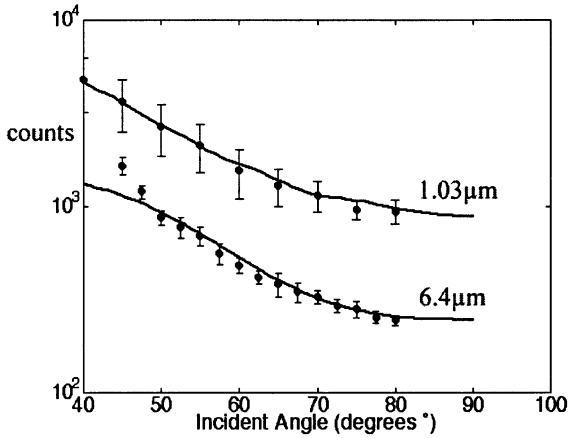

Fig. 5. Perpendicular polarized light scattered by a sphere of diameter 6.4 μm and a sphere of diameter 1.03 μm. The NA of the objective lens was 0.55. Scaling factor fs $= 2.5$ for the 6 μm sphere and 1.8 for the 1 μm.

collection model. θ_i defines the incident ray's angle relative to the normal to the glass slide. β and ϕ are, respectively, the deviation angle and azimuthal angle of scattering by the microspheres. An objective lens with an aperture specifies a solid angle of collection, θ_{coll}. All the photons scattered within the cone of collection of the objective lens are collected by the objective lens.

The deviation angle β depends on the angles θ, θ_i, and ϕ

$$\beta = \cos^{-1}\left(-\sin\theta_i \sin\theta \cos\phi + \cos\theta_i \cos\theta\right). \qquad (1)$$

Rays scattering from a single particle distribute themselves according to a phase function $p(\beta, \phi)$, determined by the particle size and predicted by Mie theory. To calculate the light contribution at a point A, we need to consider not only the scattering angle θ, but also the rotation ϕ of the azimuth angle. We used the Stokes vector formalism. The incident Stokes vector $S = [I \quad Q \quad U \quad V]$ is projected into the scattering plane using a rotational matrix $R[\phi]$ [10]; the scattering at angle θ is regulated by a scattering matrix $M[\theta]$ whose elements are given by Mie theory; finally, the S vector is rotated $[-\phi]$ in order to evaluate it in the original frame of reference. To account for the analyzer orientation, a polarizer Mueller Matrix P is added to the equation.

In our model, these steps are conducted for every incident angle θ_i and $0 < \phi < 2\pi$, where the scattered angle β is given by (1), so at a point A the contribution of the scattered Stokes vector is given by the vector A

$$A = \int_0^{2\pi} \int_0^{\theta_c} PR(-\phi)M(\beta)R(\phi)Sd\theta d\phi. \qquad (2)$$

The first term of the resulting vector $A(1)$ is the intensity at a point A.

Fig. 4 shows the predicted behavior for a sphere of diameter 2 μm for different NA of the collecting objective lens. The typical periodicity, or hilly behavior, of the angular scattering curve of Mie theory is noticeably lost as the NA increases (0.0548,0.1 0.3, and 0.55). The peaks and valleys average to an almost shapeless form for NA $= 0.55$, which was the NA of the objective lens used in the initial experiments.

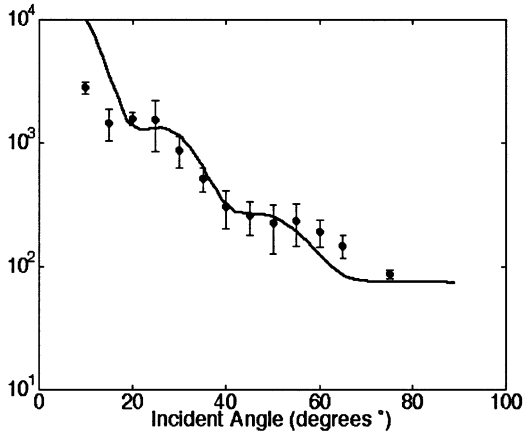

Fig. 6. Parallel polarized light scattered by one sphere of diameter 2.03 μm. Aperture 400 μm. Scaling factor fs $= 0.1$.

To obtain a higher Mie scattering signature, the NA of the collecting objective lens was decreased by restricting the collection area of the lens. We positioned a small aperture of diameter D in front of the pupil of the objective lens. The new effective NA is given by the equation

$$NA = \frac{D}{2f}$$

where f is the lens focal length. Our aperture was positioned on the front surface of the lens. Restricting the NA of the objective lens caused a loss in image resolution, as predicted by the Rayleigh criterion. Despite these artifacts, we were able to distinguish single isolated spheres and to evaluate the angular information. Three effective NA were tested: 0.55, 0.0952 ($D = 400$ μm), and 0.0548 ($D = 230$ μm).

III. Results

Figs. 5–8 show experimental results (dark circles) and the model fit (dark line). The model was scaled with a simple multiplicative scale factor (fs) to fit the data. Data are expressed in counts. The data start at the critical angle and end at 80°. Values below the critical angle, in which the unscattered incident beam light contributes to the image, were not considered.

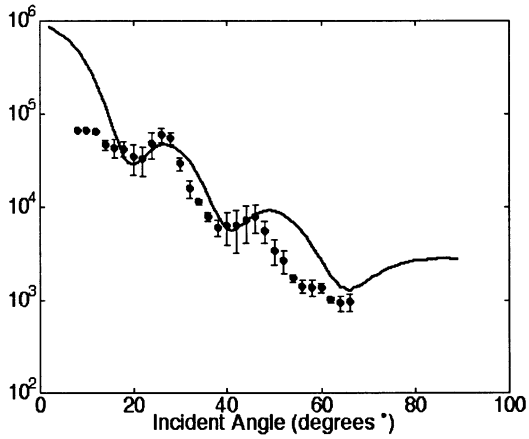

Fig. 7. Perpendicular polarized light scattered by one sphere of diameter 2.03 μm. Aperture 230 μm. Scaling factor fs $= 2.1$.

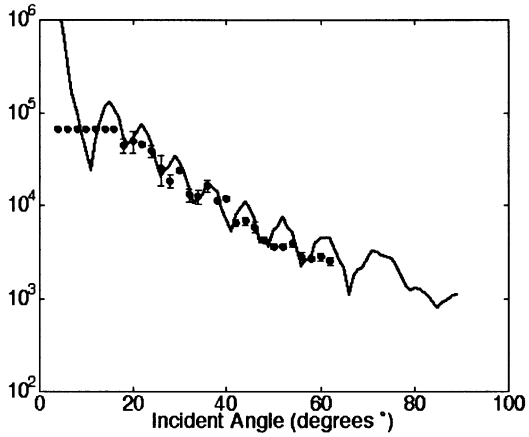

Fig. 8. Perpendicular polarized light scattered by one sphere of diameter 6.4 μm. Aperture 230 μm. Scaling factor fs $= 1.1$.

Fig. 5 shows the results of experiments for two sizes of spheres, using a 0.55 NA. For both experiments, we polarized the source and oriented the detector analyzer perpendicular to the scattering plane. As predicted by the model, the typical Mie scattering shapes averaged out, and we obtained only a smooth exponential decay.

Fig. 6 shows the results obtained with a pinhole diameter equal to 400 μm. In this case, the polarizer and analyzer were oriented parallel to the scattering plane.

Figs. 7 and 8 show results for an aperture of diameter 230 and spheres of diameter 2.03 μm and 6.4 μm. More periodic behavior is seen. The variation from the model could be explained in part by an inaccuracy in the measurement of the lens pupil diameter. The real objective diameter might, in fact, be larger than that established with the pinhole diameter. The real objective NA would then be larger than assumed.

The first two points of Fig. 7 and the first seven points of Fig. 8 are lower than expected because of camera saturation.

A. Fitting of the Data

All data sets were fitted with a least squares fitting for different particle sizes. To do the fitting we first generated multiple curves with our model. To generate the curves, we used different

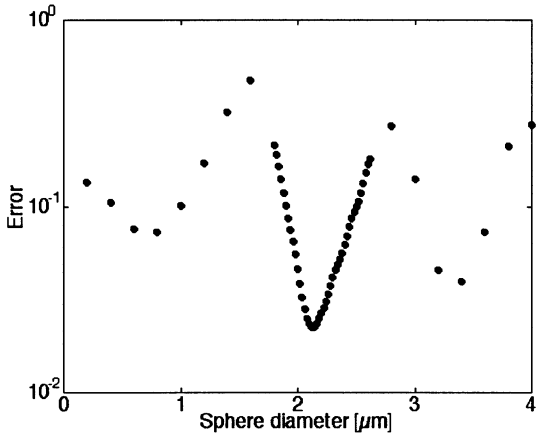

Fig. 9. Results of least squares fitting for 2.03 μm diameter microspheres. A minimum error was measured for three spheres on the same experiment. The average diameter for these fits was 2.11 μm and their standard deviation was 0.06 μm. Two other minima are visible in the figure, this could constitute a problem when trying to determine the particle size.

particle sizes in increments of 0.01 μm, the model NA was the same NA as in the experiment. We normalized both the model and the experimental data by their respective value at $\theta_c + 10°$, we added the 10° to avoid the artifacts that we noticed, for the experimental values, at angles close to θ_c. Every normalized curve was then fitted to the experimental data set and the error was plotted versus the particle size to which the fitted curve corresponded. For every size, three different experimental data sets were fitted. A typical result for a fit to an experiment conducted with 2.03 μm spheres and an aperture equal to 230 μm is shown in Fig. 9. A minimum is clearly observable close to 2 μm. A mean and standard deviation sphere size was calculated using the fitting results for three different particles.

For 2.03 μm spheres, the mean calculated radius was 2.11 μm with a standard deviation of 0.06 μm.

Similar fitting implemented for the 6.4 μm micro sphere gave a mean diameter of 6.34 μm and a standard deviation of 0.07 μm. Going to a larger NA increased the error in the fit as we expected. Fitting a 2.03 μm with an aperture equal to 400 μm 2 minima of equal importance were found one mean minimum at 2.96 μm with a standard deviation of 0.003 μm and one at 2.58 μm with a standard deviation of 0.03 μm. Finally, for the 1.03 μm and 6 μm spheres with a NA $= 0.55$, no clear minimum was visible.

Because one application of this technique could be sizing epithelial cell nuclei as they enter a precancerous state, we modeled the behavior of spheres whose indices of refraction were close to the nuclear index of refraction $n = 1.43$ [4], in a $n = 1.37$ medium for an objective lens with small NA ($D = 230\,\mu$m) (see Fig. 10). Epithelial cells are typically 5–10 μm in diameter [11]. The model showed a clear difference between the predicted behavior for 5 μm-diameter spheres and 15 μm-diameter spheres.

IV. Discussion

We have introduced a new method to evaluate a sphere particle size using an inverted microscope and a goniometric

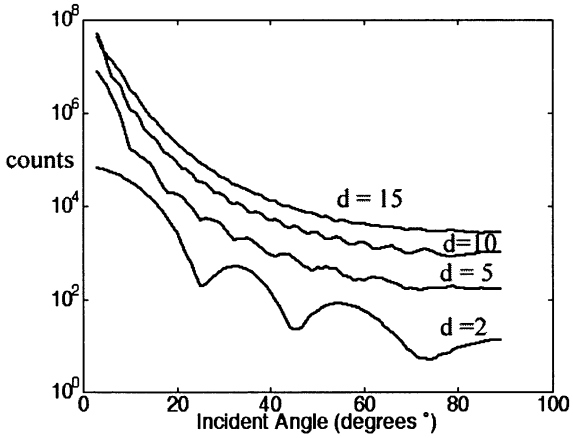

Fig. 10. Modeled behavior of perpendicular polarized light scattering from a modeled nucleus. The relative index of refraction was 1.036. The nucleus size varied from 2 to 15 μm. Because epithelial cell nuclei range from 5 to 10 μm in diameter, we can expect to be able to detect nucleus enlargement and scattering from smaller particulates such as organelles.

assembly to illuminate a scattering sample at various incident angles. We modeled the behavior of a monodisperse solution of particles, and we analyzed a range of particle from 1.03 to 6.4 μm in diameter. The first important element in this kind of measurement resides in collecting only light that has scattered from the sphere, thus, avoiding the unscattered light that has no valuable information. To do so, we took measurements only with the light source oriented at angles higher than the NA of the objective lens, this put a first restriction to the collection of light.

When a microscope objective lens of 40$\times$ and an NA equal to 0.55 was used in our measurement we obtained curves that were smooth and did not offer any particular shape apart from an exponential decay, so a sphere of 1.03 μm in diameter was easily confused with a sphere six times bigger. This was due to the fact that, in the image, we were averaging a large range of scattered rays, the only limitation being the cone of collection of the objective lens. The hilly shapes typical of certain sizes for the specific wavelength were averaged out to generate the smooth curves of Fig. 5. The solution to this problem was to decrease the objective lens cone of collection trying not to sacrifice visibility. When an aperture of 230 μm in diameter was used on the objective lens, its cone of collection had decreased of ten times, allowing a better selection of the scattered rays. The curve experimentally obtained with such an aperture allowed a better discrimination between different sizes.

We performed a least squares fit of the experimental data and only the results obtained with the small objective lens NA converged to the true size values. In the example proposed in Fig. 9 for a 2.03 μm sphere, the error of the fit showed an absolute minimum at 2.11 μm. Other relative minima were visible in the error curve at 3.3 and 0.7 μm. This could constitute a problem when no information of particle size is available *a priori*. A more refined error calculation that simply added to the least squares fit error calculation, the information of the number of relative maxima present in the model curve compared to the number of maxima present in the experimental curve, may drastically improve the size identification.

In this paper, we only considered a monodisperse solution of spheres, but we think that, given the narrow cone of collection, an optical fingerprint of the dominating particle size can also be extracted from polydisperse solutions.

We believe that one of the potential uses of this technique is to identify morphological changes in cell nuclei. The advantage of this technique would be that it can simultaneously image the cells and allow quantitative analysis of cells size.

ACKNOWLEDGMENT

The authors wish to gratefully acknowledge T. Moffitt for insightful discussions.

REFERENCES

[1] L. T. Perelman, V. Backman, M. Wallace, G. Zonios, R. Manoharan, A. Nusrat, S. Shields, M. Seiler, C. Lima, T. Hamano, I. Itzkan, J. Van Dam, J. M. Crawford, and M. S. Feld, "Observation of periodic fine structure in reflectance from biological tissue: A new technique for measuring nuclear size distribution," *Phys. Rev. Lett.*, vol. 80, pp. 627–630, 1998.

[2] V. Backman, R. Gurjar, K. Badizadegan, R. Dasari, I. Itzkan, L. T. Perelman, and M. S. Feld, "Polarized light scattering spectroscopy for quantitative measurement of epithelial cellular structures *in situ*," *IEEE J. Select. Topics Quantum Electron.*, vol. 5, pp. 1019–1027, July/Aug. 1999.

[3] R. Richards-Kortum, R. Drezek, K. Sokolov, and K. Gossage, "Reflectance spectroscopy with polarized light: Is it sensitive to cellular and nuclear morphology," *Opt. Expr.*, vol. 5, no. 13, p. 302.

[4] M. Canpolat and J. R. Mourant, "Particle size analysis of turbid media with a single optical fiber in contact with the medium to deliver and detect white light," *Appl. Opt.-OT*, vol. 40, no. 22, pp. 3792–3799.

[5] J. D. Khaydarov and B. Ovryn, "Measurement of three-dimensional velocity profiles in a thin channel flow using forward scattering particle image velocimetry (FSPIV)," in *Proc. ASME Fluids Eng. Div. Summer Meeting*, 1996, pp. 4403–408.

[6] B. Ovryn, T. Wright, and J. D. Khaydarov, "Measurement of three-dimensional velocity profiles using forward scattering particle image velocimetry (FSPIV) and neural net pattern recognition," in *Proc. SPIE*, vol. 2546, 1995, pp. 112–124.

[7] B. Kachar, "Asymmetric illumination contrast: A method of image formation for video light microscopy," *Science*, vol. 227, pp. 766–768, 1984.

[8] F. Bretshneider and P. F. Teunis, "Reduced-carrier single-sideband microscopy: A powerful method for the observation of transparent microscopical objects," *J. Microscopy*, pt. 2, vol. 175, pp. 121–134, 1994.

[9] G. Greenberg, "Direct 3-D imaging using a multiple oblique microscope," *Scanning*, vol. 16, no. 4, pp. 248–249, 1994.

[10] S. Chandrasekhar, *Radiative Transfer*. Oxford, U.K. and New York: Oxford Univ. Press and Dover, 1960.

[11] G. Karp, *Cell and Molecular Biology, Concepts and Experiments*. New York: Wiley, 1996.

Jessica C. Ramella-Roman received the Laurea degree in electrical engineering, with a minor in bioengineering, from the University of Pavia, Pavia, Italy, in 1993. She is currently pursuing the Ph.D. degree in electrical engineering at the Oregon Health Science University, Portland.

She was a Visiting Student at the Laboratoire de Physique des Lasers, University of Paris XIII, Paris, France in 1992–1993. She worked in the semiconductor field for five years before returning to academia. Her interests are in polarized light imaging and modeling and spectroscopic diagnostic of port wine stains and skin lesions.

Paulo R. Bargo received the B.S. degree in electrical engineering from the National Institute of Telecommunications, Santa Rita do Sapucai, Brazil, in 1992, the M.S. degree in electrical engineering from the University Vale do Paraiba, Sao Jose dos Campos, Brazil, in 1995. He is currently pursuing the Ph.D. degree in electrical engineering from the Oregon Health and Science University, Portland.

He was a visiting student at the G.R. Harrison Spectroscopy Laboratory, Massachusetts Institute of Technology, Cambridge, in 1996, and an Assistant Professor at the University Vale do Paraiba during 1996–1998. His research interests include biomedical optics, photodynamic therapy, biomedical instrumentation, optical diagnostics, and spectroscopy.

Scott A. Prahl received the B.S. degree in applied physics from the California Institute of Technology, Pasadena, in 1982, and the Ph.D. degree in biomedical engineering from the University of Texas, Austin, in 1988.

He is currently a Senior Scientist at the Oregon Medical Laser Center, Providence, St. Vincent Medical Center, Portland. He is also an Assistant Professor of biomedical engineering in the OGI School of Science and Engineering, Oregon Health and Science University, Portland. His current research interests include photon migration, laser thrombolysis for stroke, molecularly imprinted polymers, and coagulation techniques for hemostasis during liver surgery.

Steven L. Jacques received the B.S. degree in biology and the M.S. degree in electrical engineering from the Massachusetts Institute of Technology, Cambridge, in 1975 and 1979, respectively, and the Ph.D. degree in biophysics and medical physics from the University of California, Berkeley, 1985.

He has been working in the field of biomedical optics and laser-tissue interactions for 19 years. He was with the Wellman Labs for Photomedicine, Massachusetts General Hospital, Boston, for five years and with the University of Texas M. D. Anderson Cancer Center, Houston, for eight years. For the past six years, he has been a Professor of biomedical engineering and a Research Associate Professor of dermatology at the Oregon Health and Science University, Portland, and a Senior Scientist at the Oregon Medical Laser Center, Providence St. Vincent Medical Center, Portland. His research has been funded by grants from the National Institute of Health, the National Science Foundation, the Department of Education, the Air Force Office of Scientific Research, and the Whitaker Foundation.